Vortex phase diagram of $HgBa_2Ca_2Cu_3O_{8+\delta}$ thin films from magnetoresistance measurements

Wan-Seon Kim, W. N. Kang, Mun-Seog Kim, and Sung-Ik Lee
National Creative Research Initiative Center for Superconductivity and Department of Physics, Pohang University of Science and Technology, Pohang 790-784, Republic of Korea
(Received 29 November 1999; revised manuscript received 13 January 2000)

We have investigated the resistive behavior of $HgBa_2Ca_2Cu_3O_{8+\delta}$ thin films from the Arrhenius form $\rho(T,H)=\rho_0\exp(-U_0/T)$. The effective activation energy, $U_e\equiv -d(\ln\rho)/d(1/T)=U_0-TdU_0/dT$, is compared with the model based on thermally activated flux flow (TAFF), where $U_0(T,H)=U_0(0,H)(1-T/T_c)^{3/2}$. In a limited temperature region, $T^*<T<T_{ff}$, $\rho(T)$ follows the TAFF behavior, and this region is regarded as the pinned liquid state. In the TAFF region, all curves for the effective activation energy for different magnetic fields converge onto one line with a scaling factor $U_0(0,H)$ proportional to $1/H$. The crossover temperature, T_{ff}, separates TAFF from free flux flow. The intermediate region, $T_{irr}<T<T^*$, where T_{irr} is the temperature of irreversibility, is called the critical state and is between a pinned liquid and a vortex solid. Finally, based on these analyses, we determine the dynamic vortex phase diagram for different pinning behaviors of the vortex.

The vortices within an extremely clean superconductor can move freely even for a small driving current. Once flux lines move with velocity **v**, an electric field $\mathbf{E}=\mathbf{B}\times(\mathbf{v}/c)$ is induced, and thereby the power dissipates. However, in a material containing structural defects or impurities, the movement of the vortex can be blocked by such disorders. Owing to the vortex pinning effect, the vortex phase diagram in the H-T plane is divided by the vortex-melting or the vortex-glass lines. Between the true superconducting vortex-solid state and $H_{c2}(T)$, there exists a vortex-liquid state with activated or diffusive vortex movement. The activated behavior originates from thermally activated flux flow (TAFF) for $T<U_0$ while the diffusive behavior originates from the free-flux flow (FF) for $T>U_0$, where the activation energy U_0 is in temperature units. The resistivity due to TAFF has been studied extensively for high-temperature superconductors, such as $Bi_2Sr_2CaCu_2O_8$ (Bi-2212) (Ref. 1) and $YBa_2Ca_3O_7$ (YBCO).[2–5]

The vortex dynamics between the two very different superconductors YBCO and Bi-2212 have shown quite interesting features. In the case of Bi-2212, due to a strong two-dimensional nature, the TAFF region extends to significantly lower temperatures. In this low-temperature region U_0, which is proportional to $H_c^2\xi^3$, is a slowly varying function of temperature. Palstra *et al.*[1,4] measured $\rho(T)$ for Bi-2212 and obtained the temperature-independent activation energy U_0 in a limited temperature region. On the other hand, for YBCO, the TAFF region is very narrow, and the variation of $U_0(T)$ is large for this less anisotropic superconductor. The study of the transport for the intermediate anisotropic superconductor $HgBa_2Ca_2Cu_3O_{8+\delta}$ (Hg-1223) will be quite interesting because it will provide a bridge between the behavior of a highly anisotropic superconductor and that of a less anisotropic superconductor.

In this paper, we present an analysis of the activation energy $U_0(T,H)$ for Hg-1223 thin films. Systematic transport measurements for Hg-1223 have not yet been reported due to a lack of high-quality samples. However, we were able to deposit high-quality thin films, so transport measurements and an analysis of U_e based on the TAFF model were possible. The analysis showed various behaviors, such as the FF, the TAFF, the critical-state, and the vortex solid behaviors. At a certain temperature $T=T^*$, an abrupt increase in the effective activation energy with decreasing temperature was observed. In addition, the scaling of the activation energy was also obtained. Based on these analyses, the dynamic vortex phase diagram of the moderately anisotropic superconductor Hg-1223 was determined.

In the TAFF region, the longitudinal resistivity is represented by the form $\rho=\rho_0\exp(-U_0/T)$. Because it can be described by $\ln\rho\simeq -U_0/T$, many studies have assumed that the slope of the Arrhenius curve is directly equal to the activation energy U_0, corresponding to the derivative form $-d(\ln\rho)/d(1/T)$. Generally, however, U_0 depends on the temperature. Thus, the slope of a simple Arrhenius plot does not correspond to the actual activation energy U_0. As the activation energy is typically proportional to $H_c^2\xi^3$, it can be represented by

$$U_0(T,H)=U_0(0,H)(1-T/T_c)^{\beta}, \tag{1}$$

where the field dependency is included in $U_0(0,H)$ and β is an exponent. Among the several models for $U_0(T,H)$, we will consider two models, one by Tinkham[3] and the other by Yeshurun and Malozemoff.[2] According to the former, $U_0(t,H)=U_0(0,H)(1-t^2)(1-t^4)^{1/2}$ whereas in the latter, $U_0(t,H)=U_0(0,H)(1-t)^{3/2}$, where $t=T/T_c$ is a reduced temperature. Yeshurun and Malozemoff assumed two things. First, $\xi(T)$ and $H_c(T)$ are in the clean-limit forms, i.e., $H_c=1.73H_{c0}(1-T/T_c)$ and $\xi\sim\xi_0(1-T/T_c)^{-1/2}$. Second, if κ is large, then ξ^3 should be replaced by ξa_0^2, where a_0 is the flux-lattice spacing. With those assumptions, then $\beta=3/2$ is natural. Once we accept the form of U_0 in Eq. (1) and define $U_e\equiv -d(\ln\rho)/d(1/T)$, then

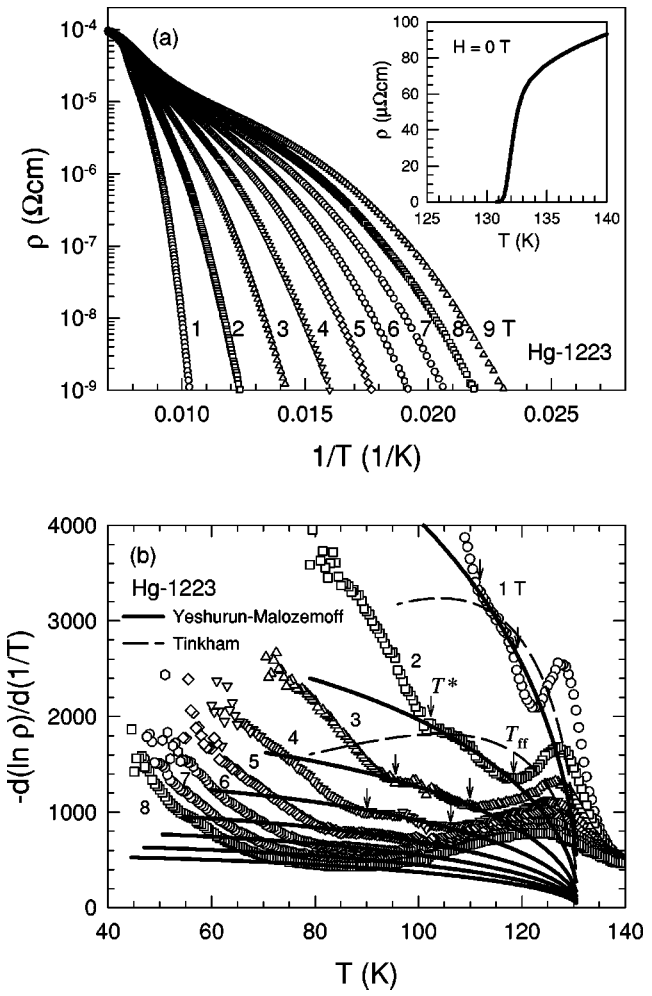

FIG. 1. (a) Arrhenius plots of $\rho(T)$ are shown for various magnetic fields parallel to c axes of the Hg-1223 thin films. Inset shows the $\rho(T)$ at $H=0$ T, where $T_c=131$ K. (b) The temperature dependence of the slope of the Arrhenius curve $U_e=-d(\ln\rho)/d(1/T)$ is plotted with open symbols for various fields. The solid lines are calculated by using Eq. (3) with $\beta=3/2$. The values of U_e in the limited temperature region $T^*<T<T_{ff}$ are well described by the theoretical calculation (solid lines) suggested by Yeshurun and Malozemoff. The dashed lines represent the calculation done by using Tinkham's form. T^* and T_{ff} are explained in the text in detail.

$$U_e(T,H)=U_0(T,H)-TdU_0(T,H)/dT \tag{2}$$

$$=U_0(0,H)(1-T/T_c)^{\beta}\left[1+\frac{\beta(T/T_c)}{1-T/T_c}\right]. \tag{3}$$

This equation reduces to Eq. (1) in the limit $T/T_c\rightarrow 0$.

High-quality Hg-1223 thin films were grown with Re-doped $Ba_2Ca_2Cu_3O_x$ precursor powder by using pulsed-laser deposition followed by post annealing of Hg. The as-grown film on (100) $SrTiO_3$ exhibited a zero-resistance transition at 131 K with a narrow transition width of ~ 2 K after oxygen annealing at 340 °C, as shown in the inset of Fig. 1(a). From the magnetization measurement, the critical current density was estimated to be $\sim 10^6 A/cm^2$ at 77 K in zero field. The x-ray-diffraction pattern indicated highly c-axis-oriented thin films with phase purities more than 95%. The scanning-electron microscopy analysis showed that the surface morphology of the films was well-connected platelike crystals. The details were reported elsewhere.[6,7]

Figures 1(a) and 1(b) show the Arrhenius plots of $\rho(T,H)$ for external fields from 1 to 9 T and the slope $-d(\ln\rho)/d(1/T)$ as functions of temperature, respectively. The external magnetic fields were applied parallel to the c axis of the thin film. In Fig. 1(a), one can see that the slope strongly depends on the temperature. This feature is in sharp contrast to the case of Bi-2212. As Palstra *et al.*[1,4] reported previously, for Bi-2212, the slope is nearly constant in the range of $\rho\sim 10^{-1}$–10^{-4} $\mu\Omega$ cm, meaning the temperature-independent U_0. Because Bi-2212 has a strong two-dimensional nature, the vortex-liquid region is extended significantly to the low-temperature side. Hence, TAFF behavior also appears in the low-temperature region where the activation energy is nearly constant because $U_0\sim H_c^2\xi^3$. On the other hand, Hg-1223 is known to be a relatively less anisotropic material with $\gamma\simeq 30-50$.[8,9] Therefore, in order to describe the resistive behavior of Hg-1223 in the TAFF region, the temperature dependence of U_0 should be considered. A similar feature in the YBCO compounds was reported by Zeldov *et al.*[5]

In Fig. 1(b), all the experimental curves (open symbols) show a decrease in U_e as T goes below T_c ($=131$ K), followed by an increase as the temperature continues to decrease. However, below a certain temperature T^*, indicated by the arrow, this increase becomes very rapid. Using previously described theoretical models, we calculated U_e and compared the result to the experiment. The solid lines in this figure represent U_e calculated with $U_0(t,H)=U_0(0,H)(1-t)^{3/2}$ suggested by Yeshurun and Malozemoff. The dashed lines represent U_e calculated with Tinkham's form $U_0(t,H)=U_0(0,H)(1-t^2)(1-t^4)^{1/2}$. The analyses show that the Yeshurun-Malozemoff model with $\beta=3/2$ is more appropriate for describing the experimental data in the limited temperature interval $T^*\leqslant T\leqslant T_{ff}$. T_{ff} is the temperature where flux flow freely. Thus, the deviations of the data from the theoretical curves for $T>T_{ff}$ are due to the fact that the thermal energy exceeds the activation energy. Even though the temperature range is different for each fixed magnetic field, there surely exists a limited temperature region in which the experimental data will match the results of the TAFF theory proposed by Yeshurun and Malozemoff. This is different from the case of YBCO with a lower anisotropy ratio, in which Zeldov *et al.*[5] found that Tinkham's form[3] was valid. Based on this analysis, we could classify the magnetoresistance behavior into three different parts: an intermediate-temperature region which is well described by the Yeshurun-Malozemoff model[2] (TAFF) and near T_c (FF) and low-temperature regions (critical state) where the data depart from the Yeshurun-Malozemoff model.

If we properly normalize $U_e(T)$, all the curves in the TAFF regime may converge onto one curve; we call this a scaling behavior. This scaling behavior of the effective activation energy U_e with the scaling factor $U_0(0,H)$ is plotted in Fig. 2. The scaling of U_e originates from the fact that the pinning potential has the same nature for different vortex densities and temperatures. All of the experimental values converge onto the theoretical curve, which provides more

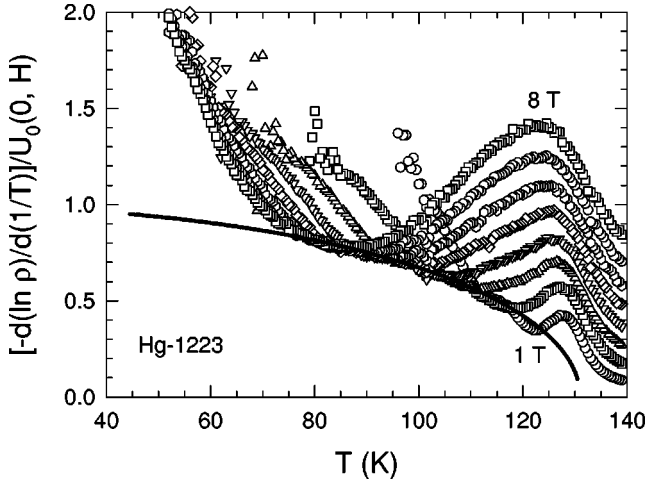

FIG. 2. The scaling behavior of the effective activation energy U_e is shown. The scaling factor is $U_0(0,H)$ in Eq. (3). The solid lines are calculated scaling curves based on the Yeshurun-Malozemoff model.

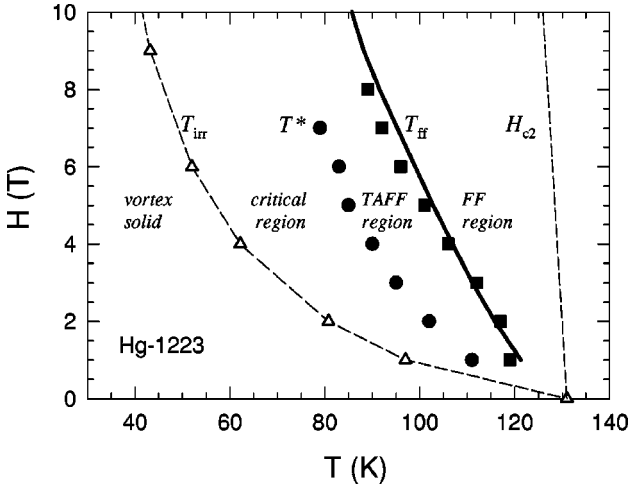

FIG. 4. The vortex phase diagram for Hg-1223 thin films. The calculated T_{ff} is represented by a solid line while the experimentally determined T_{ff} and T^* are represented by solid circles and solid squares, respectively. The T_{irr} line (open triangles) is defined by the criterion that $\rho = 10^{-9}$ Ω cm at each temperature, where the dashed line is simply a guide line. H_{c2} is deduced from $dH_{c2}/dT \simeq -2$ T/K near T_c.

confidence for the conclusion that the Yeshurun-Malozemoff model is a reasonable one for describing the TAFF behavior for Hg-1223.

The scaling factor $U_0(0,H)$ as a function of the external magnetic field is plotted in Fig. 3. The value of $U_0(0,H)$ varies systematically in H and is proportional to $H^{-\alpha}$ with $\alpha = 1.1$, as predicted by the Yeshurun-Malozemoff model (where, $\alpha = 1$). The predicted temperature and field dependences of U_0 in the Yeshurun-Malozemoff model are all confirmed in our experiment. For Bi-2212, similar experiments were performed by Palstra *et al.*[1,4] Their values of α for $\sim H^{-\alpha}$, with $\alpha \simeq 1/2$ for $H < 3$ T and $\alpha \simeq 1/3$ for $H > 3$ T, where H was parallel to the c axis, are quite different from the predicted α of 1.

On the other hand, for $HgBa_2CaCu_2O_{6+\delta}$,[10] the field and the temperature dependences of $U_e(T,H)$ were $U_e(H) \sim H^{-1}$ and $U_e H \sim (1 - T/T_c)^{\beta}$ with $\beta \simeq 1.1$. Thus, we are able to confirm that the behavior of the effective activation energy is associated with the anisotropy of the material. The magnitude of the effective activation energy for Hg-1223, as shown in Fig. 1(b), is around 10^3 K, which is between the value of 10^2 K for Bi-2212 and the value of 10^4 K for YBCO.[4] The pinning strength of the Hg-1223 superconductor turns out to be between those of Bi-2212 and YBCO.

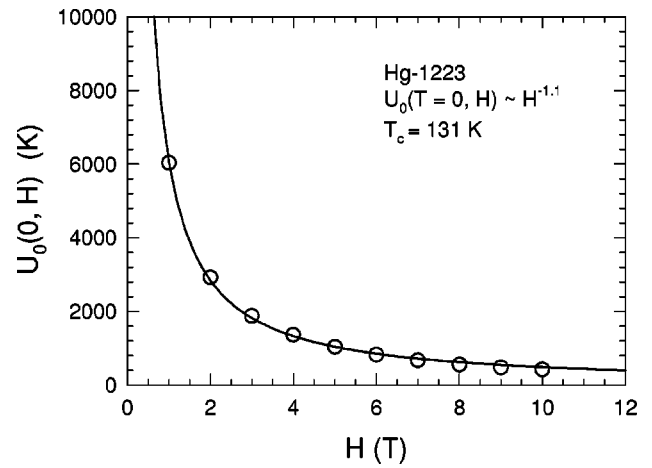

FIG. 3. The field dependence of $U_0(0,H)$ is plotted with open circles. The solid line is a fitting curve for $\sim H^{-\alpha}$, where $\alpha = 1.1$.

From Fig. 1(b) and the analysis of that figure, we are able to draw the phase diagram of the vortex states for Hg-1223, as shown in Fig. 4. The boundary between TAFF and FF is easily obtained from Fig. 1(b). At T_{ff}, the activation energy U_0 starts to become comparable to the thermal energy T, and the TAFF behavior is no longer valid for $T > T_{ff}$. The theoretical boundary, the solid line, is obtained by assuming $U_0/T = 1$ and matches relatively well with the experimental results, the solid circles. This line distinguishes the activated behavior below T_{ff} from the free flux-flow behavior above T_{ff}. On the other hand, the effective activation energy begins to increase abruptly from a certain T^*, the solid squares. We infer that T^* is the crossover temperature from the TAFF to the critical region. A similar behavior was observed for Bi-2212 by Safar *et al.*,[11] who claimed that it represented a crossover from high-temperature Arrhenius to low-temperature vortex-glass behavior. Compared with T^* for Bi-2212, T^* for Hg-1223 lies at a higher temperature. For $H = 3$ T, for example, $T^* \simeq 0.7T_c$ for Hg-1223, while $T^* \simeq 0.3T_c$ for Bi-2212.[11] Consequently, the TAFF region of Hg-1223 is narrower than that of Bi-2212. However, this region is wider than that of YBCO because in the YBCO system, TAFF is difficult to find except at very high current levels.[4,5] In Fig. 4, the upper critical field $H_{c2}(T)$ is roughly estimated by assuming that the slope $dH_{c2}/dT \simeq -2$ T/K near T_c, and T_{irr} is defined as the temperature where the resistivity becomes 10^{-9} Ω cm.

In summary, the vortex dynamics in the superconducting Hg-1223 thin film was studied by means of resistivity measurements in the field range of $1\ \text{T} \leqslant H \leqslant 9$ T. It was demonstrated that the vortex phases in the vortex-liquid state are divided into the TAFF and the FF regions. In the TAFF

region, the effective activation energy $U_e(T,H)$ was obtained and was well described by $U_0(T,H) \sim H^{\alpha}(1-T/T_c)^{\beta}$ with $\beta = 1.5$. The $U_e(T)$ curves at different external fields scaled onto a single universal curve with the scaling parameter $\alpha = -1.1$. These results are consistent with the predictions of the Yeshurun-Malozemoff model. An abrupt increase in U_e with decreasing temperature was observed at the lower boundary of the TAFF region. This behavior might indicate a crossover in the vortex dynamics from TAFF to critical behavior. Finally, from the above analyses, the vortex phase diagram of Hg-1223 was drawn.

This work was supported by Creative Research Initiatives of the Korean Ministry of Science and Technology.

[1] T. T. M. Palstra, B. Batlogg, L. F. Schneemeyer, and J. V. Waszczak, Phys. Rev. Lett. **61**, 1662 (1988).
[2] Y. Yeshurun and A. P. Malozemoff, Phys. Rev. Lett. **60**, 2202 (1988).
[3] M. Tinkham, Phys. Rev. Lett. **61**, 1658 (1988).
[4] T. T. M. Palstra, B. Batlogg, R. B. van Dover, L. F. Schneemeyer, and J. V. Waszczak, Phys. Rev. B **41**, 6621 (1990).
[5] E. Zeldov, N. M. Amer, A. Gupta, M. W. McElfresh, and R. J. Gambino, Appl. Phys. Lett. **56**, 680 (1990).
[6] W. N. Kang, R. L. Meng, and C. W. Chu, Appl. Phys. Lett. **73**, 381 (1998).
[7] W. N. Kang, Sung-Ik Lee, and C. W. Chu, Physica C **315**, 223 (1999).
[8] C. Panagopoulos, J. R. Cooper, G. B. Peacock, I. Gameson, P. P. Edwards, W. Schmidbauer, and J. W. Hodby, Phys. Rev. B **53**, 2999 (1996).
[9] Y. C. Kim, J. R. Thompson, D. K. Christen, Y. R. Sun, M. Paranthaman, and E. D. Specht, Phys. Rev. B **52**, 4438 (1995).
[10] B. W. Kang, W. N. Kang, S. H. Yun, and J. Z. Wu, Phys. Rev. B **56**, 7862 (1997).
[11] H. Safar, P. L. Gammel, D. J. Bishop, D. B. Mitzi, and A. Kapitulink, Phys. Rev. Lett. **68**, 2672 (1992).